Journal of Alloys and Compounds 728 (2017) 404–412

Contents lists available at ScienceDirect

Journal of Alloys and Compounds

journal homepage: http://www.elsevier.com/locate/jalcom

Excellent ductility and strong work hardening effect of as-cast Mg-Zn-Zr-Yb alloy at room temperature

Dongdong Zhang [a, b], Deping Zhang [a, *], Fanqiang Bu [a], Xinlin Li [b], Baishun Li [a], Tingliang Yan [b, c], Kai Guan [a], Qiang Yang [a], Xiaojuan Liu [a], Jian Meng [a, **]

[a] State Key Laboratory of Rare Earth Resource Utilization, Changchun Institute of Applied Chemistry, Chinese Academy of Sciences, Changchun, 130022, PR China
[b] College of Material Science and Chemical Engineering, Harbin Engineering University, Harbin, 150001, PR China
[c] Harbin University of Science and Technology, Harbin, 150080, PR China

ARTICLE INFO

Article history:
Received 31 May 2017
Received in revised form
30 July 2017
Accepted 1 September 2017
Available online 5 September 2017

Keywords:
Ductility
Work hardening
Twins
Magnesium alloys

ABSTRACT

In this paper, we report a new single phase solid solution as-cast Mg-1Zn-0.4Zr-0.2Yb alloy that possesses excellent ductility ($\delta_f = 38.5\%$) and strong work hardening effect ($n = 0.38$) at room temperature. The low stacking fault energy (SFE) in Mg-1Zn-0.4Zr-0.2Yb alloy might be due to the addition of trace Yb, and the low SFE is conducive to improving the activity of basal dislocation slip, activations of non-basal dislocations slips and the formation of deformation twins during tensile deformation, eventually leading to the development of the ductility in Mg-1Zn-0.4Zr-0.2Yb alloy. The strong work hardening effect of Mg-1Zn-0.4Zr-0.2Yb alloy is due to the formation of stacking faults and deformation twins induced by low SFE, which can remarkably store dislocations, restrict dislocation motions and result in multiplication and storage of dislocations at twin boundaries.

1. Introduction

Low density, high specific strength and excellent castability make magnesium alloys very attractive as structural materials in the automotive industry [1]. However, most of magnesium alloys exhibit low ductility and poor cold workability, such as cast magnesium alloys which exhibit tensile elongations of only a few percent [2]. This severely makes the industrial applications of magnesium alloys limited compared to other non-ferrous metal. Therefore, the development of new magnesium alloys with excellent ductilities and strengths at room temperature has attracted widespread attentions in recent years [3].

Work hardening effect, characterized by work hardening rate (θ), work hardening exponent (n) and work hardening capacity (H_c), is usually studied as an exploration of plastic deformation characterization of metallic materials [1,4–9]. It is generally considered that high value of n or θ implies excellent ductility, toughness and formability, especially uniform plastic elongation at room temperature [4,5,8,9]. Thus, it is a practical way to improve both the strength and the ductility through enhancing the work hardening ability, which has been widely used in most of metallic materials [5,6,8]. The extensive investigations on work hardening are primarily gathered in the aspect that work hardening originates from the hindrance to dislocation slips by twin boundaries [1,4,8,9], nano-structured second phase particles [6,7] and high-angle grain boundaries [4,5].

It has been demonstrated that rare earth (RE) elements have a favorable effect on ductilities and strengths of magnesium alloys [10]. Ytterbium (Yb) is a heavy rare earth element, and has the second largest the atomic radius (0.194 nm) among all the rare earth elements [11]. In addition, the maximum solubility of Yb in magnesium at eutectic temperature 773 K is 3.3 wt% [11], which indicates that Yb is one of the effective solution strengthening elements in a magnesium alloy. In the magnesium alloys with RE elements addition, the research of the Mg alloys containing Yb element is very lacked [11,12]. Dobromyslov et al. [12] investigated the microstructural evolution of the Mg-3.3 wt% Yb alloy during aging at 150–225 °C and evaluated the relationship between the mechanical properties and the structure forming at aging. Yu et al. [11] reported that Yb could effectively refine microstructure and remarkably improve mechanical properties of extruded ZK60 alloy.

* Corresponding author.
** Corresponding author.
E-mail addresses: zdeping@ciac.ac.cn (D. Zhang), jmeng@ciac.ac.cn (J. Meng).

http://dx.doi.org/10.1016/j.jallcom.2017.09.016
0925-8388/

Therefore, an as-cast Mg-1Zn-0.4Zr-*x*Yb ($x = 0$, 0.2 wt%) alloys have been fabricated. The influences of trace Yb addition on the mechanical properties and work hardening effect of as-cast Mg-1Zn-0.4Zr based alloys were thoroughly investigated. The reasons of high ductility and strong work hardening effect of the Mg-1Zn-0.4Zr-0.2Yb alloy were also analyzed and discussed by microstructure observation and calculation of dislocation density.

2. Experimental procedure

The Mg-1Zn-0.4Zr-*x*Yb ($x = 0$, 0.2 wt%) alloys ingots were prepared from commercially pure Mg (99.95%), Zn (99.90%), Mg-30Zr (wt.%) and Mg-15Yb (wt.%) master alloys in an electric resistance furnace under a mixed atmosphere of gas consisting of $CO_2 + 2$ vol% SF_6 at 760 ± 5 °C. To ensure homogenization, the liquid melt was stirred 2–3 times for 10 min every time with 40–50 rpm, and then the melt was held for 30–40 min at 730 ± 5 °C. Finally, the liquid melt was poured into a steel mould preheated at 250 °C, and the castings are cooled to room temperature at atmosphere. The casting mould graph and the obtained representative casting are showed in Fig. 1.

Tensile samples with a gage section of 15 mm × 4 mm × 2 mm were machined by a wire cutting machine. The tensile properties were evaluated with an initial strain rate of 1×10^{-3} s^{-1} using an Instron 5869 test machine at room temperature. Five tensile specimens were tested in order to ensure the reliability of the experimental data. Engineering stress-strain curves come from the experimental data, but true stress-strain curves are obtained by the following equation [13]:

$$\sigma^{true} = \ln(1+\varepsilon) \quad (1)$$

$$\varepsilon^{true} = \sigma(1+\varepsilon) \quad (2)$$

where σ^{true} the true stress, ε^{true} the true strain, σ the engineer stress, ε the engineering strain. Microstructures were characterized by an optical microscope (OM, Olympus GX71), a field emission scanning electron microscopy (FE-SEM Hitachi S4800) equipped with an energy dispersive spectrometer (EDS) and a field emission transmission electron microscopy (FE-TEM FEI TECNAI G2) equipped with an energy dispersive spectrometer (EDS). Samples for both OM and SEM analyses were prepared by a mechanical polishing technique, followed by etching with a solution of 2.5 g picric acid, 35 ml ethanol, 2.2 ml acetic acid and 3ml distilled water. Thin foil specimens for TEM observation were prepared by punching 3 mm diameter discs. And these foils were further thinned via low-energy ion beam with cooling system with liquid nitrogen (milling parameters: Ar, 4.5 kV, 60 min). X-ray diffraction (XRD Bruker D8 Focus) was employed to analyze the microstructure and to determine dislocation density utilizing Cu K_α radiation ($\lambda = 0.15406$ nm) at 36 kV and 40mA (scanning range (2θ): 20°~80°, scanning rate: 2°/min). Dislocation densities on different slip planes (basal {0002}, prismatic $\{10\bar{1}0\}$, pyramidal $\{10\bar{1}1\}$ and pyramidal $\{2\bar{1}\bar{1}2\}$) were calculated from XRD peak profile analysis [14]. In addition, the linear intercept method (ASTM E112-88 standards [15]) was used to measure the grain size of samples, and a minimum of 200 grains were measured for each sample. Based on ASTM E562-11 standards [16], a point-counting procedure was used to measure the volume fraction of twins. Five OM micrographs with a magnification of 200 × were taken from each sample, and then a grid of 17 points × 21 points was superimposed on the images. The volume fraction of twins was determined by calculating the ratio of the number of points positioned within the twins to the total number of grid points.

3. Results

3.1. Microstructure

3.1.1. As-cast samples

The actual compositions of the obtained ingots were determined by inductively coupled plasma atomic emission spectroscopy (ICP-AES) and the results were shown in Table 1. XRD patterns of the alloys are presented in Fig. 2. The main phase in both Mg-1Zn-0.4Zr (ZK10) and Mg-1Zn-0.4Zr-0.2Yb (ZK10Yb) alloys is α-Mg. No other phases containing Zn or Yb can be observed due to the fact that most of Zn and Yb elements were dissolved in α-Mg matrix during solidification [11]. Optical microstructures of the two alloys are given in Fig. 3a and b. The average grain size of ZK10 is 50 ± 3 μm, which is slightly larger than ZK10Yb with the average grain size of 45 ± 2 μm. Further observation from SEM images shows that one small Zr-particle is generated in the internal of the each α-Mg grain in both two samples (Fig. 3c and d). Based on the

Table 1
Actual chemical compositions of ZK10 and ZK10Yb alloys determined by ICP-AES.

Alloys	Composition (wt.%)							
	Zn	Zr	Yb	Mg	Fe	Si	Cu	Ni
ZK10	1.08	0.42	–	Bal.	0.0043	0.0029	0.0015	0.0011
ZK10Yb	1.12	0.38	0.25	Bal.	0.0037	0.0031	0.0015	0.0024

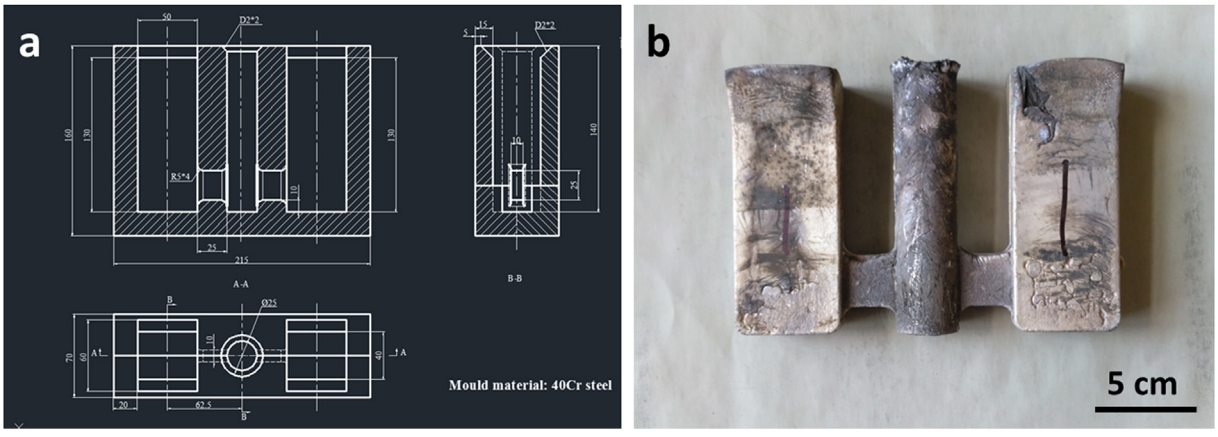

Fig. 1. (a) The casting mould graph and (b) the obtained representative casting.